MODELING THE EFFECTS OF SCREENING AEROSOLS ON PULSED DESIGNATOR SYSTEMS

Roger E, Davis and Alan C. Rishel
Science and Technology Corporation
555 Telshor Blvd., Suite 200
Las Cruces, NM 88011
Phone: (505) 521-4353
Fax: (505) 522-9062
E-mail: davis@stcnet.com

ABSTRACT

The use of high technology is now commonplace on the modem battleground. Some deployed high-technology systems use laser designators to illuminate targets. Designators are particularly effective in spectral regions unseen by the human eye because those targeted will often be unaware of impending attack. However, screening aerosols that strongly attenuate designator frequencies can defeat designator systems through concealment of targets and/or the creation of false targets.

This paper describes the Pulsed Lasers in Smoke (PULSE) model which is used to study the effects of screening aerosols on designator systems. The PULSE model provides the user with multi-layer plane parallel or Gaussian plume aerosol dispersion options. The model assumes single scattering of designator radiation in the screening aerosol. The screening aerosol is characterized by mass extinction coefficient, single-scattering albedo, and scattering phase function, all of which are functions of wavelength, The battlefield geometry is established by the designator, target, and weapon locations. Other inputs include designator pulse shape, duration, and width, target albedo, and receiver field of view.

The PULSE model output includes designator pulse shape and energy at the receiver and the location in space of the radiation returns. Results showing false target returns and stretched pulses due to their interaction with the screening aerosols are discussed.

1. INTRODUCTION

The latter part of the twentieth century has seen the development of many sophisticated weapons systems for the battlefield. Both active and passive systems arc now commonly in deployed. One type of active system employs a laser designator. Designator systems are either self-designating or require a stand-off designator to lase the intended target. One particular countermeasure used against designator systems is that of smoke and obscurants. Screening aerosols that strongly attenuate designator frequencies can defeat such systems through concealment of targets and/or the creation of false target returns. To facilitate the study of the effects of smoke/obscurants on designator signals, the Pulsed Lasers in Smoke (PULSE) simulation model was developed. This paper describes the PULSE model.

2. PULSE MODEL

The basic scenario treated by the PULSE model is illustrated by Fig, 1. The PULSE code models the interaction of a designator pulse with obscurants and a target. The model uses first principles to describe the designator-obscurant interaction. Laser pulse scattering is approximated with a single scattering algorithm. The obscurant aerosol is characterized by aerosol spatial concentration (p), single scattering albedo (ω_o), mass

extinction coefficient (α), and scattering phase function ($P(\theta,\phi)$). The single scattering albedo is defined as the ratio of the fraction of incident radiation which is scattered to the sum of the scattered and absorbed radiation. The scattering phase function is the probability distribution of scattered radiation as a function of scattering angle. The essence of the PULSE model calculations for the designator-obscurant interaction is illustrated in Fig 2.

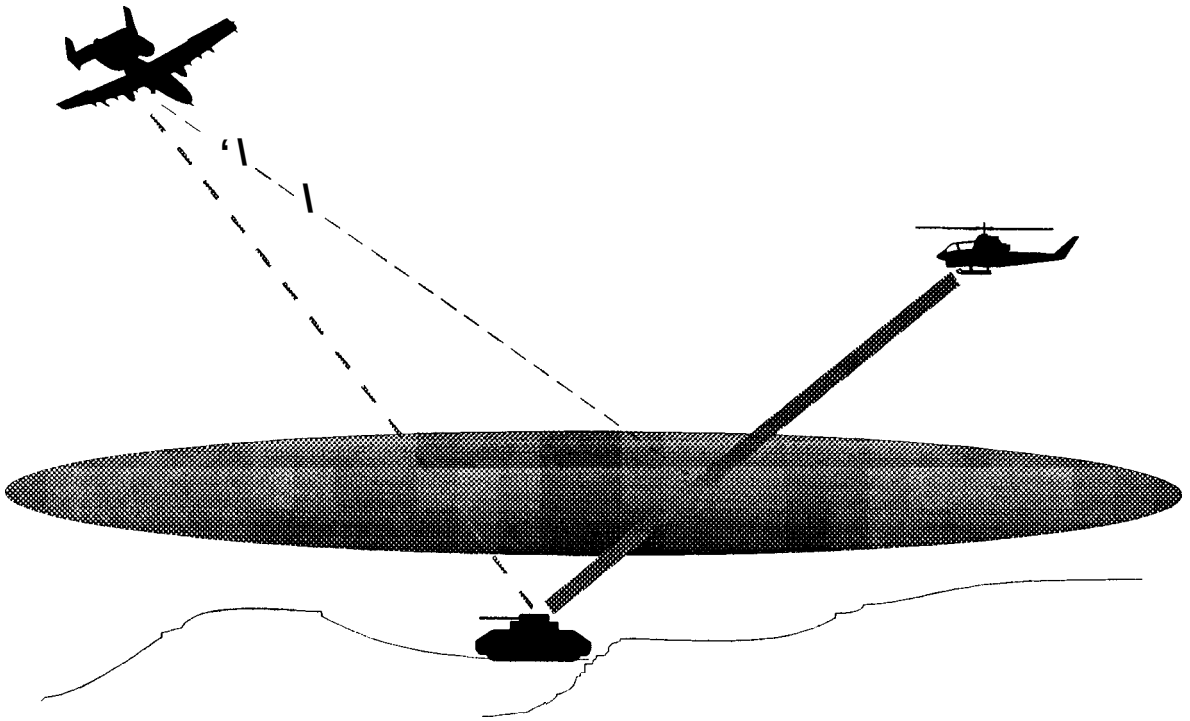

Figure 1. **PULSE model calculates the interaction of laser designators with obscurant aerosols.**

The designator-target LOS is divided into small, nominally 1 m, incremental segments. As illustrated in Fig. 2, the scattering sites are considered to be in the middle of each of these incremental segments. The pulse intensity from the designator to the scattering site is reduced by applying the Beer-Lambert law. The designator radiation "lost" from the pulse in the incremental segment is also determined from the Beer-Lambert law. The fraction of the lost radiation which is scattered is determined by the single scattering albedo for the obscurant. The single scattering albedo is, in general, wavelength dependent. The fraction of the scattered radiation which is directed toward the seeker is determined by the wavelength dependent obscurant phase function and the field geometry. Radiation scattered in all other directions or absorbed by the obscurant is ignored.

The obscurant aerosol is currently distributed by one of two methods. The first method is a stratified layer approach. Each obscurant layer is assigned its own parameters of concentration, mass extinction coefficient, single scattering albedo, and phase function. Each layer is also assigned a vertical thickness and height above the ground. This approach allows study of variable concentration and cloud "holes" along the designator-target LOS. Holes are created by assigning a layer zero concentration. The PULSE model allows 20 layers to be defined. PULSE code is written such that more layers can easily be added if required.

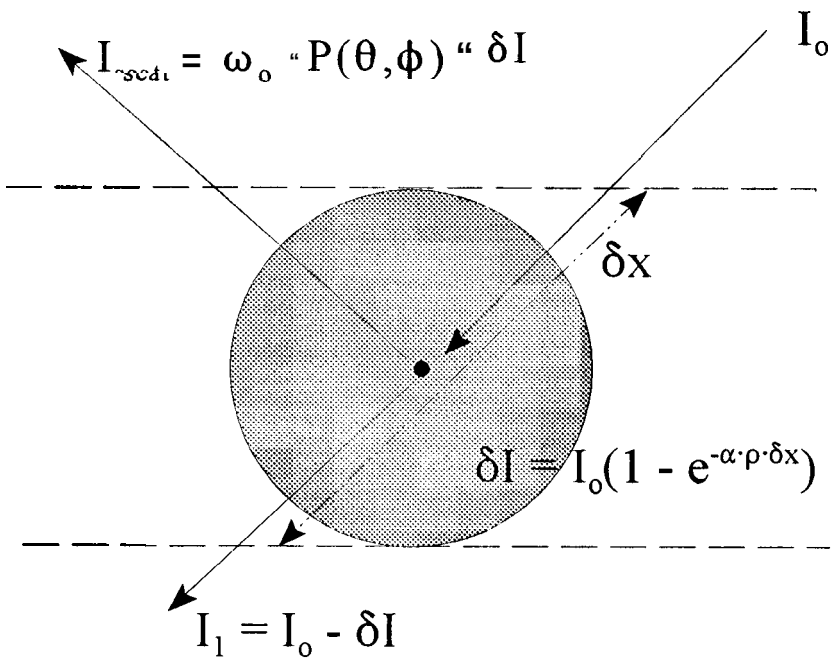

Figure 2, **Incident radiation from the top of the incremental segment is attenuated as described by the Beer-Lambert Law. The fraction of radiation scattered toward the seeker is calculated using the single scattering albedo and the phase function.**

The second option for obscurant concentration distribution a Gaussian plume model. This model allows for obscurant buoyancy, a vertical wind vector, evaporation of the fog oil as a function of downwind distance, and scavenging of obscurant material by the terrain. Both the layer model and the Gaussian model are static representations of the obscurant cloud.

The results of the PULSE model calculations are designator pulse profiles at the seeker aperture (Fig 3) as well as the spatial coordinates of scattering points in the obscurant and from the target (Fig 4). The designator-target-seeker geometry allowed by PULSE assumes that the designator and the seeker will be horizontal to or above the target.

A dynamic (time dependent) obscurant cloud algorithm is not yet verified for PULSE. However, the STATBIC (Hoock, 1994) algorithm developed by Dr. Don Hoock of the U.S. Army Research Laboratory has been included as an obscurant dissemination option in the PULSE model. This algorithm provides a time-dependent, fractal-like description of the obscurant cloud. While this algorithm has been included in the PULSE code it has not been fully verified. This option should used cautiously.

Certain "tricks" could be exercised using the aerosol static dispersions options to provide time-dependent simulations, For example, preprocessing of the weapon night path and designator location could be accomplished to create a series of look-up tables. This preprocessing approach involves manually manipulating the obscurant cloud structure for each time step during the flight. While this technique is labor intensive, it could be employed in lieu of exercising the time-dependent algorithm.

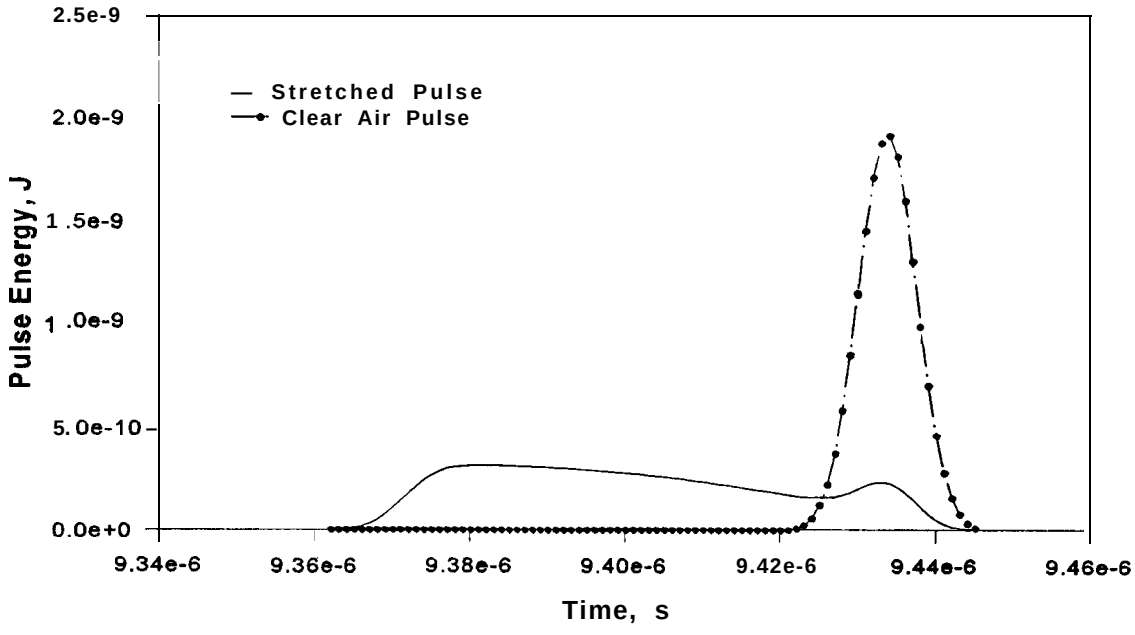

Figure 3. **The dot-dash curve represents the designator pulse reflected by the target in clear air. The solid curve is the designator pulse calculated for a Gaussian plume over the target.**

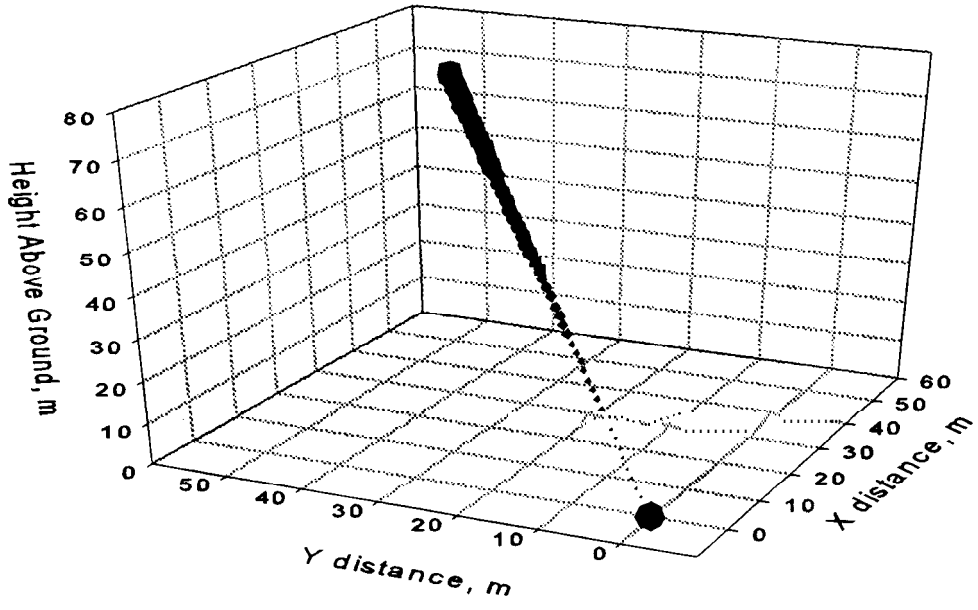

Figure 4. **Locations and relative intensities of designator energy scattered by obscurant cloud.**

The PULSE code is written in plain vanilla FORTRAN 77 with special attention paid to portability. The model is currently functional as described and has undergone extensive verification to identify and correct code errors or logic errors. Verification has included running both the layer and Gaussian distribution models for a wide range of geometries and optical depth conditions. Limited validation of the model has been accomplished (Davis and Rishel, 1997) using field data. A copy of the code can be obtained by contacting:

Dr. Hriar Cabayan (5 10) 422-8871
Lawrence Livermore National Laboratory
P.O. Box 808 (L-180)
Livermore, CA 94550

3.0 EXAMPLE PULSE RUN

The example PULSE run presented in this section is taken from a PULSE validation effort which used data acquired during the Counter Precision Guided Munitions (PGM) Srnoke/CEP/Tower (SCEPTOR) trials held at Eglin AFB in June 1994. The validation compares the PULSE model pulse profile at the seeker with the pulse profile actually recorded during the trial event. This comparative validation requires the cloud concentration information to be coincident in time with the recording of the designator profile, The PGM SCEPTOR trials, the trial data sets, and the model validation effort are documented in Davis and Rishel (1997).

Instrumentation at the PGM SCEPTOR test included transmissometers, radiometers, lidar, video cameras, meteorological instruments, and seeker head. An oscilloscope connected to the seeker head recorded the designator pulses as processed by the seeker head electronics. The seeker head, lidar, one radiometer, and one transmissometer were located at the top of a 300' meteorological tower. The target, an 8' x 10' board covered with diaper cloth, was located on the ground approximately 110 m east-north-east of the tower. The board was rotated 45° south of the designator (lidar) LOS and tilted 45° from the vertical toward the sky. The slant path distance from the top of the tower to the target was approximately 194 m.

Part of the input required by the PULSE model is the specification of obscurant concentration as a function of location along the designator-target-seeker LOS. For the model validation this information was derived from the lidar optical-depth-per-meter data. The lidar, which was used to map the obscurant cloud concentration, was also used as the laser designator for the validation data sets. Because the seeker head was co-located with the lidar at the top of the tower, a backscatter geometry was established. Using the lidar as the designator allowed the mapping of the cloud concentration along the designator-target-seeker LOS.

The obscurant layer model was selected for the PULSE validation runs. This is a reasonable approach since the cloud is "frozen" for a given pulse. The backscatter geometry allows the precise placement of the cloud segment positions and of the cloud segment concentrations at the time of designation

One of the problems encountered in performing the validation runs was the fact that the lidar information and the oscilloscope seeker head pulse profiles were not exactly time coincident. The lidar data was reported once every 3 or 4 seconds and is a 1-s average based on 16 pulses. The oscilloscope profiles were recorded on video tape, but digitized profiles for analysis were copied to files at irregular intervals with time tags only to the nearest whole second. The radiometer data shows that the concentration along a given LOS can change dramatically in a fraction of a second. Thus, the cloud structure reported by the lidar may have changed significantly from the time the seeker head pulse was recorded. Obscurant cloud lidar profile and the oscilloscope profile presented in this example are separated in time by (at least) one second.

A second problem impacting the comparative analysis was fact that the oscilloscope recorded the designator pulses after being processed by non-linear electronics in the seeker head. That is, the oscilloscope pulse profiles are non-linear in amplitude. It was learned from discussions with test engineers that no information concerning the gain switching levels was recorded and no transformation could be applied to the profiles. Therefore, the comparison between modeled pulses and observed pulses is limited in detail because the modeled pulses are linear in amplitude.

Figure 5 illustrates how concentration and path length input data was derived from the lidar cloud information. The slant path length through a cloud segment is taken to be the full width of isolated segments such as segments 1 and 4 shown in Figure 5. Specifying the width of blended segments (e.g. segments 2 and 3) is more complicated. Through some trial and error and a review of the oscilloscope profiles, it was eventually decided that some "clear air" was usually required between blends with well-defined peaks, In these cases a point halfway between the lesser peak of the blend and the minimum between the peaks was chosen. From this point a line was constructed to intersection the larger peak of the blend. One-quarter of this distance was assigned as the clear air path length between the blended segments. Allowing for this amount of clear air between the segments, the path lengths through the blended segments were determined. The optical depth integrations were performed to the minimums between the peaks.

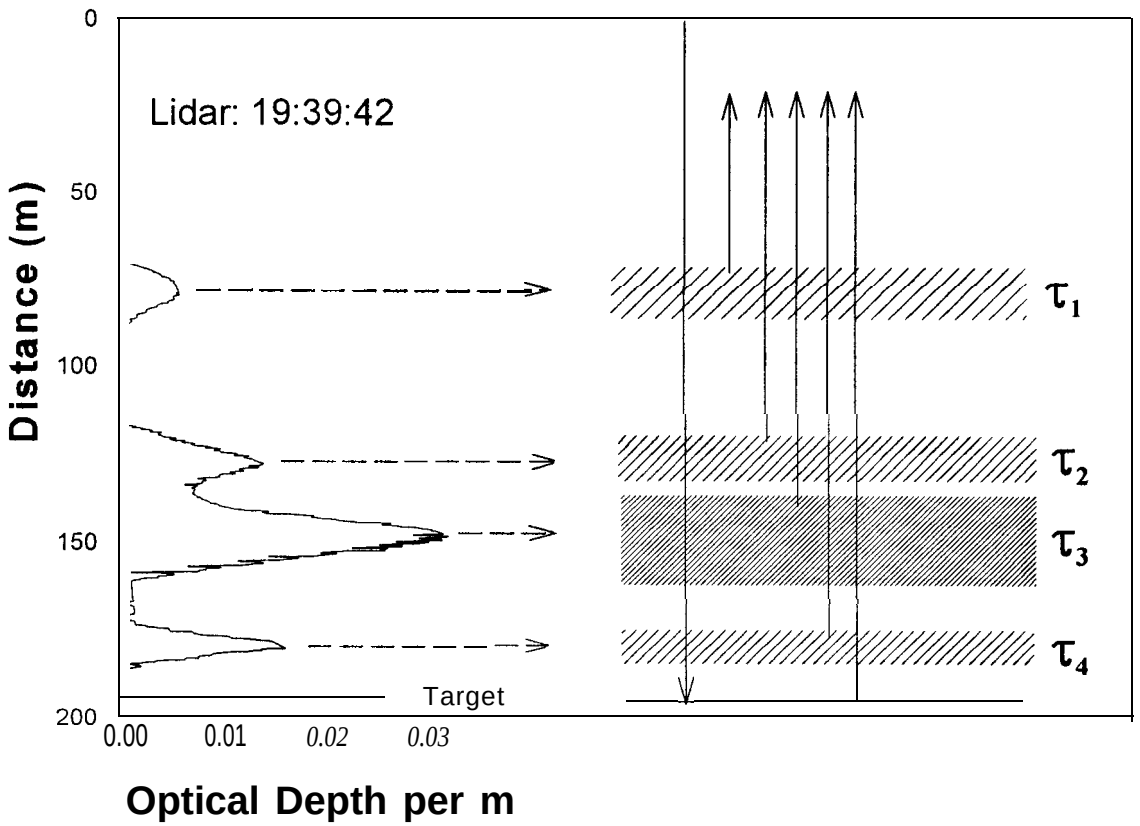

Figure 5. Optical depth, τ, and cloud segment thickness is determined from a lidar profile (left side of fig.). The optical depth for each major cloud segment is computed by integration over the segment thickness. Segment thickness is measured directly.

The locations of the cloud segments relative to the designator (and seeker in this case) were determined directly from the lidar measurements. The mean aerosol concentration in each obscurant segment, l_i, was determined by:

$$< p >_i = \frac{\tau_i \, l_i}{\alpha(\lambda)} \qquad (1)$$

where:

et(A)	=	mass extinction coefficient, m^2/g
τ_i	=	segment I total (integrated) optical depth
l_i	=	slant path distance through segment I, m

A fog oil mass extinction coefficient of 1.5 m^2/g for 1.06 pm, derived from LAS SEX (Bulk-d, et al., 1995) field transmission and nephelometer measurements, was used in eq. 1 to determine obscurant concentrations needed by the PULSE model for the example. The optical depths for the individual segments were determined by integrating the lidar optical-depth-per-m over the each segment. The slant path lengths were measured directly from the segment widths. The layer thickness for the model input was the segment slant path thickness reduced by the cosine of the lidar-target LOS as measured from the vertical.

The results of the example run are displayed in Fig. 6. Also displayed in Fig. 6 are the oscilloscope pulse profile and the lidar cloud optical-depth-per-meter data. The oscilloscope data and PULSE model profiles are presented as a function of distance rather than time. This allows a standard plot format for Fig 6. For convenience, all data sets types have been registered with the ground target position, 194 m from the lidar/seeker position at the top of the tower. The oscilloscope and PULSE model profiles maybe compared directly for features as a function of distance. The cloud structure (lidar data) features can be compared with the model profiles but the distance coordinates for model designator profile features will be expanded factor of 2 due to the test geometry. In comparing the profiles, the reader is reminded that 1) the oscilloscope profiles have been processed by non-linear seeker head electronics, 2) the modeled profiles are linear and based on lidar cloud structure data, and 3) the lidar cloud structure profiles are averages of 16 profiles and are not precisely time coincidence with the seeker head (oscilloscope) profiles.

In reviewing the results presented in Fig. 6 it is obvious that the width of the modeled pulse as reflected at the target is approximately half that of the target pulse recorded at the oscilloscope. Several factors may be responsible for this difference between the observed and modeled pulse. The most important factor is probably the fact that model assumed a flat Lambertian target perpendicular to the pulse propagation. In reality, the target was rotated approximately 45° to the lidar and approximately 45° to the horizontal. This will cause the lidar spot to become elongated on the target, resulting in a broadening of the return pulse. Secondly, it is possible that the reported pulse width of the lidar could be in error. Thirdly, the non-linear amplification of the reflected pulses by the seeker head will server to magnify the base of the return pulse. This magnification of the wings of the target return is evident in the target signature which always has a small peak (the central portion of the pulse) resting on the shoulders of the target return.

The review of the results presented in the Fig. 6 also reveals that the modeled profiles tend to have somewhat concave shapes on the trailing sides of the pulses, This signature is attributed to the Beer-Lambert treatment of the designator pulse as it traverses the obscurant medium. That is, the intensity of the pulse power is reduced as $\exp(-\tau)$ as the pulse traverses the obscurant. The reasons the oscilloscope pulses do not

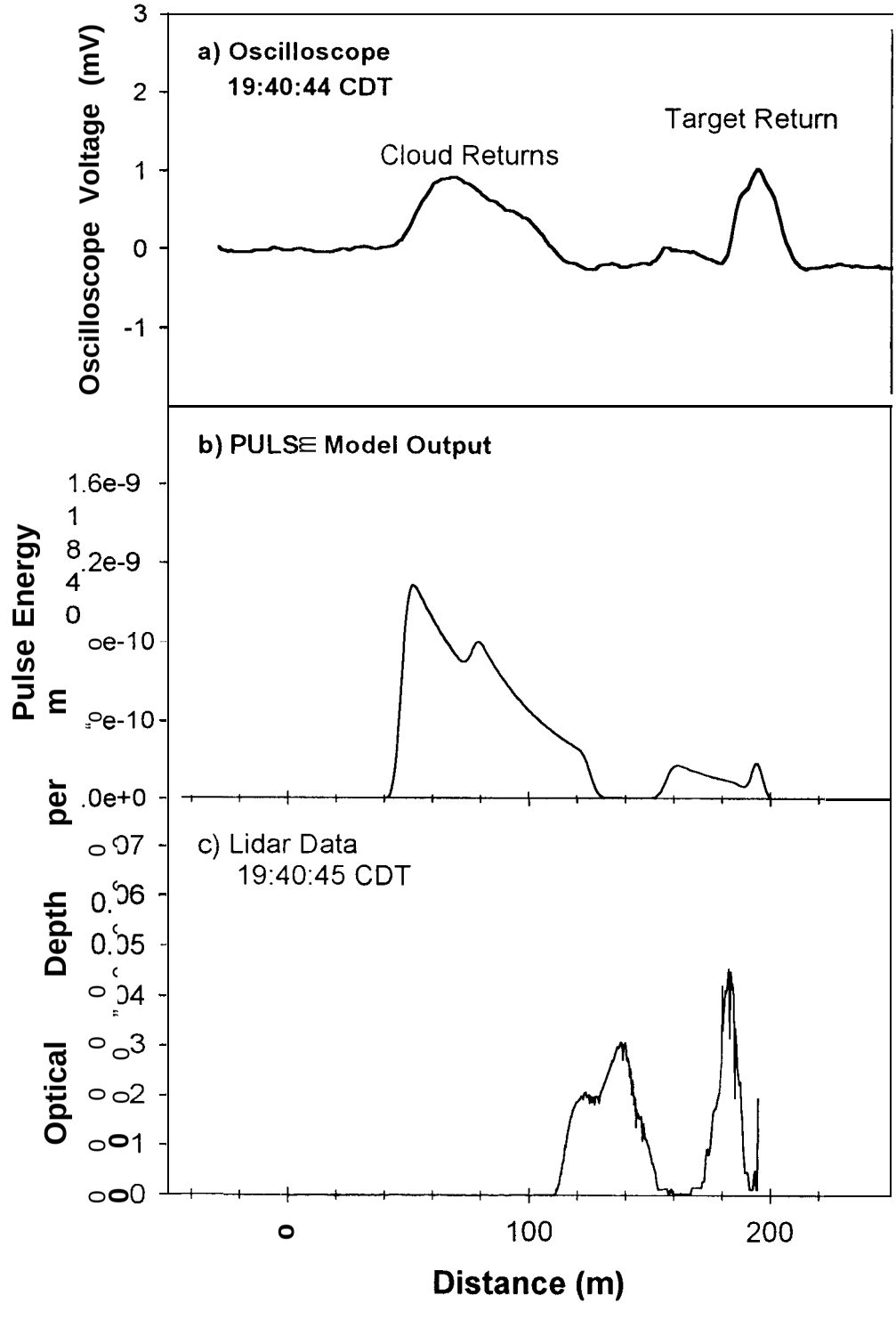

Figure 6. a) Designator profile as processed by the seeker, b) PULSE model profile at seeker aperture, and c) lidar obscurant cloud profile near time of seeker head observation.

show a distinctive concave signature include: (1) the oscilloscope profiles are processed by the non-linear seeker head electronics, and (2) the ocsilloscope profiles, unlike the PULSE model profiles, include the full effects of multiple scattering. However, the degree to which multiple scattering effects the overall profile shape is uncertain at this time.

Overall, the modeled features for the example data set compare quite favorably with the oscilloscope pulse segments. The multiple structure in the leading pulse segment is mimicked reasonably and second independent segment adj scent to the target shows the proper shape and signature. Additionally, the pulse stretching has been computed accurately.

5. SUMMARY

The PULSE model is currently operational. It is wavelength independent in the sense that the wavelength is determined by the obscurant input parameters (single scattering albedo, phase function, and mass extinction coefficient). It is also aerosol independent as long as the obscurant input parameters are available. PULSE uses either a stratified plane-parallel mode or Gaussian cloud approximation mode to distribute the obscurant cloud. Both of these modes are static in nature. A dynamic cloud distribution algorithm is available but has not been fully verified. PULSE is available (see Section 2) to interested users.

PULSE model validation is incomplete due to a lack of a comprehensive field data set. Nonetheless, as the example presented in Fig 6 shows, the PULSE model can provide a reliable and generally accurate representation of a designator pulse which has encountered an obscurant cloud.

REFERENCES

Bullard, B. R., R.E. Davis, S. Germ-d, W.G. Klimek, and R.L. Laughman, 1995: *Large-Area Smoke Screen Experiment (LASSEX), Final Report.* STC Technical Report 2910, Science and Technology Corporation, Hampton, VA 23666

Davis, R.E. and Rishel, A, 1997, *Counter PGM SCEPTOR Data Analysis and PULSE Model Validation,* STC Technical Report 3125, Science and Technology Corporation, Hampton, VA 23666

Hoock, D. W., 1994, *Theory and Field Meausrements Analysis for Verification of the STATBIC Statistical Plume Visualization Algorithm, Summary Description,* MORS Handbook, U.S. Army Research Laboratory, Battlefield Environment Directorate, White Sands Missile Range, NM 88002-5501.